Quantum Dots

DOI: 10.1002/anie.200906154

Water-Soluble Fluorescent Carbon Quantum Dots and Photocatalyst Design**

Haitao Li, Xiaodie He, Zhenhui Kang, Hui Huang, Yang Liu,* Jinglin Liu, Suoyuan Lian, Chi Him A. Tsang, Xiaobao Yang, and Shuit-Tong Lee**

Carbon nanostructures are attracting intense interest because of their many unique and novel properties. The strong and tunable luminescence of carbon materials further enhances their versatile properties; in particular, the quantum effect in carbon is extremely important both fundamentally and technologically.[1–4] Recently, photoluminescent carbon-based nanoparticles have received much attention. They are usually prepared by laser ablation of graphite, electrochemical oxidation of graphite, electrochemical soaking of carbon nanotubes, thermal oxidation of suitable molecular precursors, vapor deposition of soot, proton-beam irradiation of nanodiamonds, microwave synthesis, and bottom-up methods.[5–13] Although small (ca. 2 nm) graphite nanoparticles show strong blue photoluminescence (PL),[13] definitive experimental evidence for luminescence of carbon structure arising from quantum-confinement effects and size-dependent optical properties of carbon quantum dots (CQDs) remains scarce.

Herein, we report the facile one-step alkali-assisted electrochemical fabrication of CQDs with sizes of 1.2–3.8 nm which possess size-dependent photoluminescence (PL) and excellent upconversion luminescence properties. Significantly, we demonstrate the design of photocatalysts (TiO_2/CQDs and SiO_2/CQDs complex system) to harness the use of the full spectrum of sunlight (based on the upconversion luminescence properties of CQDs).

It can be imagined that judicious cutting of a graphite honeycomb layer into ultrasmall particles can lead to tiny fragments of graphite, yielding CQDs, which may offer a straightforward and facile strategy to prepare high-quality CQDs.[3] Using graphite rods as both anode and cathode, and NaOH/EtOH as electrolyte, we synthesized CQDs with a current intensity of 10–200 mA cm^{-2}. As a reference, a series of control experiments using acids (e.g. H_2SO_4/EtOH) as electrolyte yielded no formation of CQDs. This result indicates that alkaline environment is the key factor, and OH^- group is essential for the formation of CQDs by the electrochemical oxidation process. Figure 1a shows a transmission electron microscopy (TEM) image of CQDs with diameters within 4 nm, revealing the as-synthesized CQDs are uniform and monodisperse. By the present cutting method, the as-synthesized CQDs were consist of a mixture of different sized carbon dots. These as-synthesized CQDs were investigated under a fluorescent microscope, and different emission colors were found in the same sample. Figure 1b shows the corresponding fluorescent microscope images of CQDs in the same sample: blue, green, yellow, and brown. As CQDs were obtained by the electrochemical cutting of graphite sheets, it may be expected that the products would consist of a mixture of ultrasmall carbon dots emitting at different colors (different emission may originate from graphite sheets of different size, symmetry, and defects). Figure 1c–h shows high-resolution TEM (HRTEM) images of typical CQDs with different diameters but the same lattice spacing of around 0.32 nm, which agrees well with the <002> spacing of graphitic carbon.[2–3,14–18]

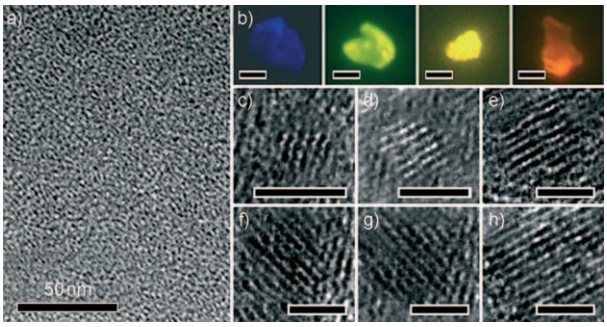

Figure 1. a) TEM image of CQDs with diameters under 4 nm; b) fluorescent microscopy images of CQDs with an excitation wavelength of 360 nm (scale bar: 50 μm); c–h) HRTEM images of typical CQDs with different diameters (scale bar: 2 nm).

To further explore the optical properties of as-synthesized CQDs, a detailed PL study was carried out by using different excitation wavelengths. Figure 2a–c shows the PL spectra of the as-synthesized CQDs obtained at current densities of 180,

[*] H. T. Li,[+] Dr. X. D. He,[+] Prof. Z. H. Kang, Y. Liu, S. Y. Lian
Functional Nano & Soft Materials Laboratory (FUNSOM) Soochow University, Suzhou, Jiangsu (P.R. China)
E-mail: zhkang@suda.edu.cn
yangl@suda.edu.cn
Prof. Z. H. Kang, Dr. H. Huang, Y. Liu, Prof. J. L. Liu
Faculty of Chemistry, Northeast Normal University
Changchun, Jilin, 130024 (China)
C. H. A. Tsang, Dr. X. B. Yang, Prof. S.-T. Lee
Center of Super Diamond and Advanced Films (COSDAF)
Hong Kong SAR (P.R. China)
E-mail: apannale@cityu.edu.hk
[+] These authors contributed equally to this work.

[**] This work was supported by the Natural Science Foundation of China (NSFC) (No. 20801010 and 20803008), the Foundation for the Authors of National Excellent Doctoral Dissertation of P.R. China (FANEDD) (No. 200929), the Research Grants Council of Hong Kong (Nos. CityU 102206 and CityU 101608).

Supporting information for this article is available on the WWW under http://dx.doi.org/10.1002/anie.200906154.

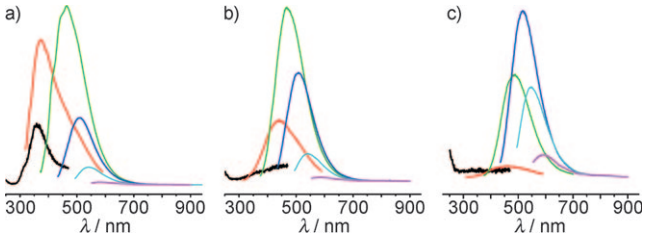

Figure 2. PL spectra of CQDs obtained at a current density of: a) 180 mA cm^{-2}; b) 100 mA cm^{-2}; c) 20 mA cm^{-2}. In these figures, the excitation wavelength for the black, red, green, blue, cyan, and pink PL lines are 240, 300, 360, 420, 500, and 580 nm, respectively.

100, and 20 mA cm^{-2}, respectively. The black, red, green, blue, cyan, and pink lines are the PL spectra for excitation at 240, 300, 360, 420, 500, and 580 nm, respectively. The PL spectra show that the current density can change the distribution of emission colors of as-synthesized CQDs, and that lower current density leads to increasing amount of CQDs emitting at longer wavelengths or warmer colors. Although the as-synthesized CQDs are a mixture of CQDs of different diameters, we can purify and separate the as-synthesized CQDs to obtain different-sized CQDs with a narrow size distribution by simple column chromatography. Further characterization supports the conclusion that different-sized CQDs yield different emission colors. Figure 3a shows optical images of CQDs of four typical sizes (their size distributions are shown in Figure S1 in the Supporting Information), illuminated under white (left; daylight lamp) and UV light (right; 365 nm, center). The bright blue, green, yellow, and red PL of CQDs is strong enough to be easily seen with the naked eye. Figure 3b shows the corresponding emission spectra; the red, black, green, and blue lines are the PL spectra for blue-, green-, yellow-, and red-emitting CQDs, respectively. A detailed study revealed that the PL properties vary sharply with CQD size (Figure 3c): small CQDs (1.2 nm, center) give UV light emission (about 350 nm, Figure S2a), medium-sized CQDs (1.5–3 nm) give visible light emission (400–700 nm), and large CQDs (3.8 nm, center) give near-infrared emission (about 800 nm, Figure S2b).

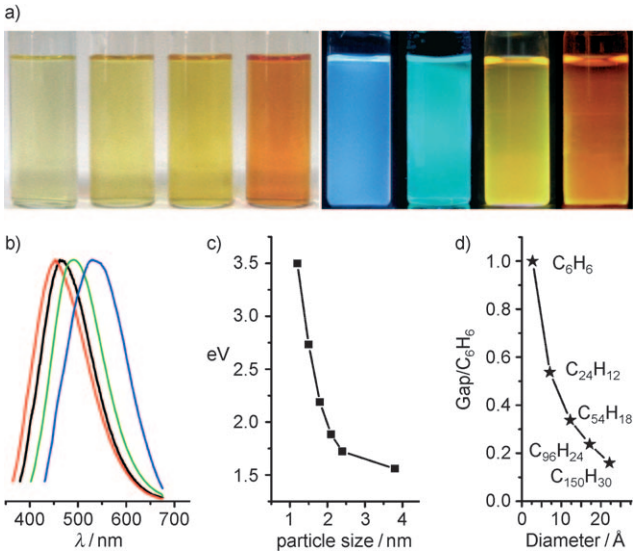

Figure 3. a) Typical sized CQDs optical images illuminated under white (left; daylight lamp) and UV light (right; 365 nm); b) PL spectra of typical sized CQDs: the red, black, green, and blue lines are the PL spectra for blue-, green-, yellow-, and red-emission CQDs, respectively; c) relationship between the CQDs size and the PL properties; d) HOMO–LUMO gap dependence on the size of the graphitene fragments.

Further characterization studies provided convincing evidence for the graphite fragment structure of the as-synthesized CQDs. Typical UV/Vis absorption spectra of CQDs are shown in Figure S3 (see the Supporting Information). The peak at 250–300 nm represents a typical absorption of an aromatic π system, which is similar to that of polycyclic aromatic hydrocarbons.[5–13,19] Raman spectra of the CQDs are shown in Figure S4 (see the Supporting Information). The peak at 1580 cm^{-1} (G band) corresponds to the E_{2g} mode of the graphite and is related to the vibration of sp^2-bonded carbon atoms in a two-dimensional (2D) hexagonal lattice. The D band at around 1360 cm^{-1} is associated with the vibrations of carbon atoms with dangling bonds in the termination plane of disordered graphite or glassy carbon.[1–4,14–18] The infrared (IR) spectrum of CQDs is shown in Figure S5 (see the Supporting Information). The peaks at about 3000, 1600, and 1500 cm^{-1} correspond to the C=C stretch of polycyclic aromatic hydrocarbons. The peaks at about 1700 cm^{-1} indicate the existence of carbonyl (C=O) groups, while the peaks at about 1719, 1203, and 1080 cm^{-1} are due to carboxylic groups. The peak at about 3346 cm^{-1} corresponds to the OH stretching mode.[14–16] To confirm that strong emission of CQDs should come from the quantum-sized fragment of graphite, the as-synthesized CQDs were treated by hydrogen plasma to remove the surface oxygen from the graphite surface. A series of control experiments showed no obvious change of the PL spectra of CQDs before and after hydrogen plasma. Figures S4 and S5 (see the Supporting Information) show the Raman and IR spectrum of CQDs before (Figures S4a and S5a) and after (Figures S4b and S5b) hydrogen plasma treatment. The insensitivity of the Raman spectra to hydrogen plasma treatment suggests that the graphite fragment structure of CQDs remained largely intact after the removal of most of the oxygen by hydrogen plasma.

To further confirm and explain that the strong emission comes from the quantum-sized graphite fragment of CQDs, we performed theoretical calculations to investigate the relationship between luminescence and cluster size.[20] Figure 3d shows the dependence of HOMO–LUMO gap on the size of the graphene fragments. As the size of the fragment increases, the gap decreases gradually, which is in agreement with our previous study,[20] and the gap energy in the visible spectral range can be obtained from graphene fragments with a diameter of 14–22 Å, which agrees well with the visible light emission of CQDs with diameters of less than 3 nm. Thus, we can conclude that the strong emission of CQDs comes from the quantum-sized graphite structure itself instead of the carbon–oxygen surface.

Significantly, the as-obtained CQDs can freely disperse in water with transparent appearance without further ultrasonic dispersion, and exhibit good photostability, that is, luminescence properties and appearance remains unchanged after storing for one year in air at room temperature. The quantum yield of CQDs with yellow emission was estimated to be about 12% by calibrating against rhodamine B in ethanol.[21–22] Remarkably, CQDs were shown to possess clear upconversion PL properties besides exhibiting strong luminescence in UV-to-near-infrared range. Figure 4 shows the PL

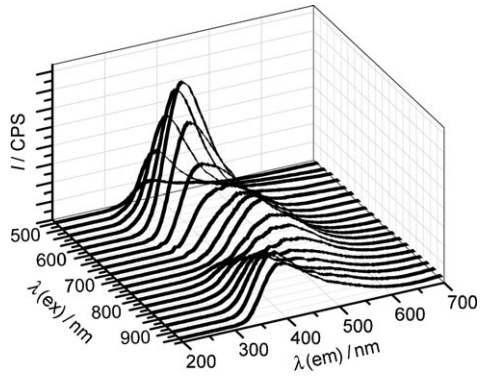

Figure 4. Upconverted PL properties of CQDs.

spectra of CQDs excited by long-wavelength light (from 500 to 1000 nm) with the upconverted emissions located in the range from 325 to 425 nm. This upconverted PL property of CQDs should be attributed to the multiphoton active process similar to previous reported carbon dots.[10a] These results suggest that CQDs may be used as a powerful energy-transfer component in photocatalyst design for applications in environmental and energy issues. TiO_2 offers potentially a facile and inexpensive method for removing environmental pollutants relating to wastewater, polluted air, and spilled water.[23–27] However, a major obstacle to its effective utilization lies in the inefficient use of sunlight or visible light as irradiation source, because less than 5% of sunlight is usable or captured by undoped TiO_2 because of its large intrinsic band gap.[23,24] In view of the upconversion properties of CQDs, we expected that combining CQDs with catalytic TiO_2 in a composite system for photocatalysis would realize the efficient usage of the full spectrum of sunlight. We used the degradation reaction of methyl blue (MB) to evaluate the photocatalytic activity of the TiO_2/CQDs and SiO_2/CQDs photocatalysts. Figure 5a,b shows the scanning electron microscopy (SEM) images of as-prepared photocatalysts for SiO_2/CQDs and TiO_2/CQDs, respectively. The insets show the corresponding HRTEM images of SiO_2/CQDs and TiO_2/CQDs particles, indicating that CQDs are attached to the surfaces of the TiO_2 or SiO_2 nanoparticles (TiO_2 NPs, SiO_2 NPs). After the solution containing the TiO_2/CQDs (SiO_2/CQDs) and MB (50 mg L^{-1}) was irradiated by visible light for 25 min (15 min for SiO_2/CQDs), reduction of MB was almost complete (ca. 100%). Figure 5c plots the MB concentration versus reaction time, from which we can observe that the process of photodegradation is efficient. In control experi-

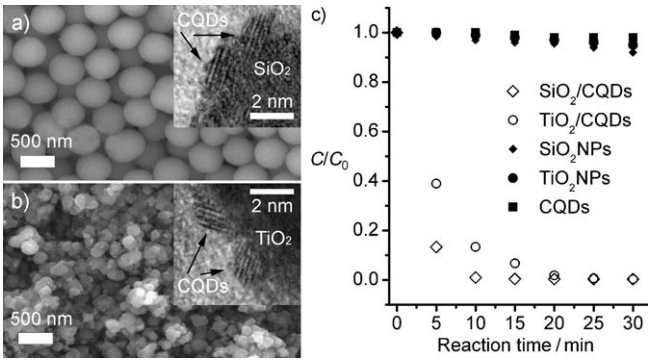

Figure 5. a,b) SEM image of photocatalysts for SiO_2/CQDs and TiO_2/CQDs; insets show the corresponding HRTEM images; c) relationship between MB concentration and reaction time for different catalysts: SiO_2/CQDs, TiO_2/CQDs, SiO_2 NPs, TiO_2 NPs, and CQDs.

ments using only pure TiO_2 or SiO_2 without CQDs as photocatalysts, no or little (< 5% for TiO_2, < 10% for SiO_2) reduction of MB was observed, showing that CQDs are necessary for efficient photodegradation under visible light. In contrast, under the same conditions, reduction of MB was nearly 0% when pure CQDs was used as the catalyst, which indicates that the excellent photocatalytic activities of TiO_2/CQDs and SiO_2/CQDs should be attributed to the interaction between CQDs and TiO_2(or SiO_2) in present catalyst system.

We explain the photocatalytic reaction process as follows (Figure 6). When the TiO_2/CQDs or SiO_2/CQDs nanocom-

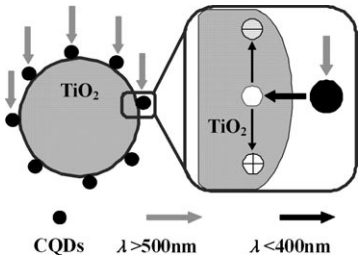

Figure 6. Possible catalytic mechanism for TiO_2/CQDs under visible light.

posite photocatalyst is illuminated, the CQDs absorb visible light, and then emit shorter wavelength light (325 to 425 nm) as a result of upconversion, which in turn excites TiO_2 or SiO_2 to form electron/hole (e^-/h^+) pairs.[25–27] The electron/hole pairs then react with the adsorbed oxidants/reducers (usually O_2/OH^-) to produce active oxygen radicals (e.g. $\cdot O^{2-}$, $\cdot OH$), which subsequently cause degradation of the dyes (MB).[23–28] Significantly, when CQDs are attached to the surface of the TiO_2 or SiO_2, the relative position of the CQDs band edge permits the transfer of electrons from the TiO_2or SiO_2 surface, allowing charge separation, stabilization, and hindered recombination.[29] The electrons can be shuttled freely along the conducting network of the CQDs.[29] The longer-lived holes on the TiO_2 or SiO_2, then, account for the higher activity of this complex photocatalyst.[29]

The as-obtained CQDs can freely disperse in water with transparent appearance without further ultrasonic dispersion, and exhibit good photostability, that is, luminescence properties and appearance remains unchanged after storing one year in air at room temperature. The excellent stability of aqueous colloids is attributed to the electrostatic stabilization (the surfaces of CQDs are passivated by COOH and OH groups).[30] This kind of graphite-based CQDs with strong and stable PL would offer great potential for a broad range of applications, including biosensors, biomedical imaging, and light-emitting diodes (LEDs).[5,10,25,27] Furthermore, the upconverted PL properties of CQDs may provide a new way to design and synthesize novel photocatalysts (through the combination of CQDs and different nanospecies, such as ZnO, Fe_2O_3, WO_3, Au, Cu, and Pt) for photo-assisted catalytic reactions.[26,27]

In summary, we have demonstrated a facile one-step alkali-assisted electrochemical synthesis of high-quality CQDs, which exhibit stable and strong photoluminescence (quantum yield about 12%). By combining free dispersion in water, size-dependent optical properties, and upconverted PL properties, CQDs may provide a new type of fluorescent markers as well as a new approach to high-efficiency catalyst design for applications in bioscience and energy technology.

Experimental Section

All chemicals were purchased from Sigma–Aldrich. In a typical experiment, the electrolyte of the electrochemical process was prepared by mixing ethanol/H_2O (100 mL; volume ratio = 99.5:0.5) with a suitable amount (0.2–0.4 g) of NaOH. By using graphite rods (diameter about 0.5 cm) as both anode and cathode, we synthesized CQDs with a current intensity in the range of 10–200 $mA\,cm^{-2}$. Typically, the rate of production of CQDs was about 10 mg per hour for each setup.

CQDs were separated by column chromatography. Firstly, the raw CQDs solution was treated by adding a suitable amount of $MgSO_4$ (5–7 wt%), stirred for 20 min, and then stored for 24 h to remove the salts and water. Afterwards, the purified CQDs solution was separated by silica-gel column chromatography with a mixture of petroleum ether and diethyl ether as the developing solvent.

TiO_2/CQDs and SiO_2/CQDs nanocomposites were synthesized by a typical sol–gel method. Firstly, for TiO_2/CQDs, tetrabutyl titanate (0.5 mL) was dissolved in ethanol (20 mL) and then water (9 mL) and ammonia (5 mL; 28%) were added with stirring. The mixture was left to age for 12 h, and then the samples were collected by centrifugation and dried in an oven at 80 °C for 6 h. TiO_2 nanoparticles were prepared by calcining the above sample at 500 °C for 1 h. Secondly, TiO_2 nanoparticles (0.05–0.1 g) was added to CQDs solution (5 mL) with stirring for 10 min and dried in an vacuum oven at 80 °C for 12 h to give the TiO_2/CQDs nanocomposite. SiO_2/CQDs catalyst was produced in the same manner by using tetraethyl orthosilicate (TEOS) in place of tetrabutyl titanate.

Photocatalytic degradation of methyl blue (MB) was carried out in a 100-mL conical flask containing 50 $mg\,L^{-1}$ MB solution and a suitable amount (10 mg) of TiO_2/CQDs and SiO_2/CQDs nanocomposite as catalyst. A 300 W halogen lamp was used for illumination. MB was determined spectrophotometrically at $\lambda_{max} = 605$ nm.

TEM and HRTEM images of CQDs were obtained with a FEI/Philips Techai 12 BioTWIN transmission electron microscope and a CM200 FEG transmission electron microscope, respectively. The normal TEM samples were prepared by dropping CQDs solution onto a copper grid with polyvinyl formal support film and dried in air. The FTIR spectrum of CQDs was obtained with a Nicolet 360 spectrometer. SEM images of TiO_2/CQDs and SiO_2/CQDs nanocomposite were obtained with Philips XL30 instrument. The PL study was carried out on a Fluorolog-TCSPC luminescence spectrometer, and UV/Vis spectra were obtained with an Aglient 8453 UV/Vis diode array spectrophotometer.

Our calculations were preformed with the SIESTA code based on density functional theory. Basis sets with double zeta and polarization function and the Lee–Yang–Par functional of the generalized gradient approximation were adopted. Such an approach has been shown to offer high accuracy and high efficiency, particularly for the study of hydrogen-terminated silicon systems.

Received: November 2, 2009
Revised: March 9, 2010
Published online: May 11, 2010

Keywords: carbon · heterogeneous catalysis · photophysics · quantum dots

[1] S. Iijima, *Nature* **1991**, *354*, 56.
[2] D. S. Bethune, C. H. Kiang, M. S. Devries, G. Gorman, R. Savoy, R. Beyers, *Nature* **1993**, *363*, 605.
[3] Z. H. Kang, E. B. Wang, L. Gao, S. Y. Lian, M. Jiang, C. W. Hu, L. Xu, *J. Am. Chem. Soc.* **2003**, *125*, 13652.
[4] Z. H. Kang, E. B. Wang, B. D. Mao, Z. M. Su, L. Gao, S. Y. Lian, L. Xu, *J. Am. Chem. Soc.* **2005**, *127*, 6534.
[5] a) Y-P. Sun, B. Zhou, Y. Lin, W. Wang, K. A. S. Fernando, P. Pathak, M. J. Meziani, B. A. Harruff, X. Wang, H. Wang, P. G. Luo, H. Yang, M. E. Kose, B. Chen, L. M. Veca, S-Y Xie, *J. Am. Chem. Soc.* **2006**, *128*, 7756; b) S. L. Hu, K. Y. Niu, J. Sun, J. Yang, N. Q. Zhao, X. W. Du, *J. Mater. Chem.* **2009**, *19*, 484.
[6] a) J. Zhou, C. Booker, R. Li, X. Zhou, T. K. Sham, X. Sun, Z. Ding, *J. Am. Chem. Soc.* **2007**, *129*, 744; b) Q. L. Zhao, Z. L. Zhang, B. H. Huang, J. Peng, M. Zhang, D. W. Pang, *Chem. Commun.* **2008**, 5116; c) J. Lu, J. X. Yang, J. Z. Wang, A. Lim, S. Wang, K. P. Loh, *ACS Nano* **2009**, *3*, 2367.
[7] a) X. Xu, R. Ray, Y. Gu, H. J. Ploehn, L. Gearheart, K. Raker, W. A. Scrivens, *J. Am. Chem. Soc.* **2004**, *126*, 12736; b) A. B. Bourlinos, A. Stassinopoulos, D. Anglos, R. Zboril, V. Georgakilas, E. P. Giannelis, *Chem. Mater.* **2008**, *20*, 4539.
[8] S.-J. Yu, M.-W. Kang, H.-C. Chang, K.-M. Chen, Y.-C. Yu, *J. Am. Chem. Soc.* **2005**, *127*, 17604.
[9] a) M. Bottini, C. Balasubramanian, M. I. Dawson, A. Bergamaschi, S. Belluci, T. Mustelin, *J. Phys. Chem. B* **2006**, *110*, 831; b) H. Zhu, X. L. Wang, Y. L. Li, Z. J. Wang, F. Yang, X. R. Yang, *Chem. Commun.* **2009**, 5118.
[10] a) L. Cao, X. Wang, M. J. Meziani, F. Lu, H. Wang, P. G. Luo, Y. Lin, B. A. Harruff, L. M. Veca, D. Murray, S-Y. Xie, Y. P. Sun, *J. Am. Chem. Soc.* **2007**, *129*, 11318; b) R. Liu, D. Wu, S. Liu, K. Koynov, W. Knoll, Q. Li, *Angew. Chem.* **2009**, *121*, 4668; *Angew. Chem. Int. Ed.* **2009**, *48*, 4598.
[11] H. Liu, T. Ye, C. Mao, *Angew. Chem.* **2007**, *119*, 6593; *Angew. Chem. Int. Ed.* **2007**, *46*, 6473.
[12] A. B. Bourlinos, A. Stassinopoulos, D. Anglos, R. Zboril, M. Karakassides, E. P. Giannelis, *Small* **2008**, *4*, 455.
[13] L. Y. Zheng, Y. W. Chi, Y. Q. Dong, J. P. Lin, B. B. Wang, *J. Am. Chem. Soc.* **2009**, *131*, 4564.
[14] Z. H. Kang, E. B. Wang, S. Y. Lian, L. Gao, M. Jiang, C. W. Hu, L. Xu, *Nanotechnology* **2004**, *15*, 490.
[15] Z. H. Kang, E. B. Wang, B. D. Mao, Z. M. Su, L. Chen, L. Xu, *Nanotechnology* **2005**, *16*, 1192.
[16] M. S. Dresselhaus, G. Dresselhaus, M. A. Pimenta, P. C. Eklund in *Analytical Applications of Raman Spectroscopy* (Ed.: M. J. Pelletier), Blackwell Science, Oxford, **1999**, chap. 9.
[17] F. Tuinstra, J. L. Koening, *J. Chem. Phys.* **1970**, *53*, 1126.

[18] J. Liu, M. Shao, X. Chen, W. Yu, X. Liu, Y. T. Qian, *J. Am. Chem. Soc.* **2003**, *125*, 8088.
[19] S. Y. Xie, R. B. Huang, L. S. Zheng, *J. Chromatogr. A* **1999**, *864*, 173.
[20] R. Q. Zhang, E. Bertran, S. T. Lee, *Diamond Relat. Mater.* **1998**, *7*, 1663.
[21] L. Li, H. F. Qian, J. C. Ren, *Chem. Commun.* **2005**, 528.
[22] A. P. Alivisatos, *Science* **1996**, *271*, 933.
[23] X. B. Chen, S. S. Mao, *Chem. Rev.* **2007**, *107*, 2891.
[24] J. Y. Li, W. H. Ma, C. C. Chen, J. C. Zhao, H. Y. Zhu, X. P. Gao, *J. Mol. Catal. A* **2007**, *261*, 131.
[25] Z. H. Kang, C. H. A. Tsang, Z. D. Zhang, M. L. Zhang, N. B. Wong, J. A. Zapien, Y. Y. Shan, S. T. Lee, *J. Am. Chem. Soc.* **2007**, *129*, 5326.
[26] Z. H. Kang, C. H. A. Tsang, N. B. Wong, Z. D. Zhang, S. T. Lee, *J. Am. Chem. Soc.* **2007**, *129*, 12090.
[27] Z. H. Kang, Y. Liu, C. H. A. Tsang, D. D. D. Ma, X. Fan, N. B. Wong, S. T. Lee, *Adv. Mater.* **2009**, *21*, 661.
[28] W. Wang, B. H. Gu, L. Y. Liang, W. Hamilton, *J. Phys. Chem. B* **2003**, *107*, 3400.
[29] Y. Yao, G. H. Li, S. Ciston, R. M. Lueptow, K. A . Gray, *Environ. Sci. Technol.* **2008**, *42*, 4952.
[30] D. Li, M. B. Müller, S. Gilje, R. B. Kaner, G. G. Wallace, *Nat. Nanotechnol.* **2008**, *3*, 101.

